M. C. JUNGER
Chief Scientist,
Cambridge Acoustical Associates, Inc.,
Cambridge, Mass.

Nonmodal Solution of Spherical Shells With Cutouts Excited by High-Frequency Axisymmetric Forces

A closed-form solution is obtained for the high-frequency response of a thin spherical shell embodying a circular cutout and excited axisymmetrically by a concentrated radial force. The solution is constructed by combining the shell response to the radial exciting force with its response to radial, tangential, and moment line loads applied along the cutout boundary, these line loads being selected to match the boundary conditions. Concise expressions for the shell response are obtained by applying the Sommerfeld-Watson transformation to the slowly converging high-frequency modal series which is thereby reduced to only two terms, viz., an exponentially decaying near-field and a standing or propagating-wave field. These two terms are in the nature of the creeping waves commonly used to formulate electromagnetic or acoustic diffracted wave fields in the short-wavelength limit. The method is illustrated for the simple case of a circular cutout with a clamped boundary, but lends itself to more complicated boundary conditions, viz., intersecting shells or wave guides. The natural frequencies and mode shapes are found from a single, characteristic equation involving trigonometric functions.

1 Extension of Watson's Creeping-Wave Formulation to Structural Vibrations

SHORT-WAVELENGTH diffraction problems are commonly solved by applying the Sommerfeld-Watson transformation to the slowly converging wave-harmonic series which is thus transformed into a rapidly converging residue or creeping-wave series. The method has been applied extensively to electromagnetic [1, 2], acoustic [3, 4], and, to a lesser extent, elastic [5] waves. The transformation was first derived approximately 50 years ago by Watson for the sphere, in his study of the transmission loss of radio waves propagating across the Atlantic. Watson showed that, for a point source located at $\theta = 0$, the wave-harmonic series for the diffracted surface field can be expressed in terms of spherical wave harmonics of complex, noninteger orders s:

$$\sum_{n=0}^{\infty} \frac{(n + \frac{1}{2})P_n(\cos\theta)}{Z(\Omega, n)} = -\frac{i}{2}\oint_{C_1+C_2} \frac{sP_{s-\frac{1}{2}}(-\cos\theta)}{\cos s\pi Z(\Omega, s)}\,ds \quad (1a)$$

where $(C_1 + C_2)$ is a clockwise contour around the positive real axis, Fig. 1. Ω is a dimensionless frequency, specifically, for Watson's problem, the circumference of the earth measured in electromagnetic wavelengths. The zeros of $\cos s\pi$ at $s = n + \frac{1}{2}$ give rise to simple poles. The integral is thus evaluated as a residue series which equals precisely the original wave-harmonic series. The function Z is restricted in that it must not have real roots coinciding with those of $\cos s\pi$. For what follows, Z is further restricted to even functions in s.

The contour is now deformed into a counterclockwise contour comprising the semicircular arc C_{R+} and the line integrals $(C_3 + C_2)$. The semicircular integral C_{R+} vanishes as $|s| \to \infty$. The integrand in $(1a)$ being odd in s, the line integral C_3 above the negative real axis equals its mirror image C_1. Hence, the counterclockwise contour integral $(C_{R+} + C_3 + C_2)$ is equivalent to the original contour integral $(C_2 + C_1)$. The new contour integral can be evaluated as $(2\pi i)$ times the residues at the complex zeros s_j of $Z(\Omega, s)$, where $\mathrm{Im}(s_j) > 0$:

$$\sum_n = -\pi \sum_{s=s_j} \frac{sP_{s-\frac{1}{2}}(-\cos\theta)}{\cos(s\pi)\partial Z(\Omega, s)/\partial s}, \qquad \theta \neq 0 \quad (1b)$$

It is found that $0(s_j) = 0(\Omega)$ and that s_j has comparable imaginary and real components. Watson's residue or creeping-wave series is effectively a series in negative powers of frequency or more precisely, of the radii of curvature of the diffracting surface measured in terms of wavelengths. It is therefore most efficient

Presented at the Sixth U. S. National Congress of Applied Mechanics, Harvard University, Cambridge, Mass., June 15–19, 1970.
Discussion of this paper should be addressed to the Editorial Department, ASME, United Engineering Center, 345 East 47th Street, New York, N. Y. 10017, and will be accepted until January 20, 1971. Discussion received after the closing date will be returned. Manuscript received by ASME Applied Mechanics Division, January 19, 1970; final revision, March 13, 1970.

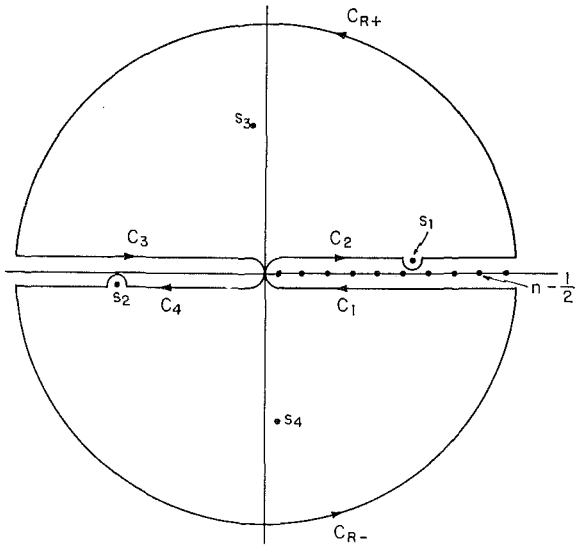

Fig. 1 Contours of integration in Sommerfeld-Watson transformation

precisely in the high-frequency range where the wave-harmonic formulation converges slowly. The creeping-wave solution is, like the wave-harmonic formulation, an infinite series. In the high-frequency range, the hypergeometric functions in (1) can be written asymptotically as

$$P_{s-\frac{1}{2}}(-\cos\theta) = \frac{2^{1/2}}{(\pi s \sin\theta)^{1/2}} \cos\left[s(\pi-\theta) - \frac{\pi}{4}\right] + 0(s^{-3/2}), \quad |s| \sin\theta \gg 1 \quad (2)$$

Expressing the cosine in (2) and $\cos(s\pi)$ in (1) in terms of exponentials, the diffracted field is displayed as traveling waves which are exponentially damped as they propagate around the sphere, since $\mathrm{Im}(s_j) > 0$. At $\theta = \pi$, the hypergeometric function in (1b) rises to a maximum of unity which embodies the focusing of the diffracted waves at the antipode. At $\theta = 0$, where $-\cos\theta = -1$, the hypergeometric functions are singular. Thus a drawback of Watson's solution, which did not interfere with his original purpose, is that the residue series cannot, by itself, represent the field in the vicinity of the source.

This limitation does not bear on the high-frequency solutions of sperical [6], and cylindrical [7] elastic shells, obtained by extending the Sommerfeld-Watson technique from wave-harmonics series to normal-mode series representing the forced vibrations of elastic shells. In this case, the denominator Z in (1a) possesses a finite number of roots s_j which, for vanishing structural damping, are either imaginary or real. Thus, in contrast to the wave-harmonic series of the diffracted field, the normal-mode series of the shell response is transformed into a *finite* sum of residues which, in the absence of structural damping, represent non-propagating exponentially decaying near-fields and unattenuated standing-wave fields. Furthermore the drive-point response is expressible asymptotically in closed form.

The concise display of the solution achieved with Watson's

Nomenclature

a = shell radius
c = characteristic compressional wave velocity in flat plates, $= [E/\rho(1-\mu^2)]^{1/2}$, or free-space electromagnetic or sound velocity
c_f = flexural wave velocity in flat plate
c_j = phase velocity of structural wave in shell
E = Young's modulus
F = concentrated radial drive force applied at $\theta_0 = 0$
F_R, F_T = respectively, resultant radial and tangential line force distributed uniformly along circle θ_0
$f(\theta), g(\theta, \theta_0)$ = dimensionless influence coefficients defined, respectively, in (8) and (18)
h = shell thickness
M = resultant moment excitation uniformly distributed around circle θ_0
n = index number of normal mode of complete spherical shell
$P_n(\cos\theta)$ = Legendre function of first kind
$P_n^1(\cos\theta)$ = associated Legendre function of order 1, $= -dP_n(\cos\theta)/d\theta$
P_s, P_s^1 = hypergeometric functions corresponding to P_n and P_n^1
p_a = applied radial stress
s = modal index number extended to complex, non-integer values
t_a = applied tangential stress
$u(\theta, \theta_0), w(\theta, \theta_0)$ = resultant circumferential and radial velocity components, respectively, of field point located at θ on mean surface of axisymmetrically excited, partial spherical shell with cutout along circle θ_0
$u_p(\theta), w_p(\theta)$ = circumferential and radial velocity components of complete spherical shell excited by a radial point force at $\theta_0 = 0$ (correspond to $\dot{u}$ and $\dot{w}$ in [6])
$u_T(\theta, \theta_0)$ = tangential velocity component of shell response at field point θ to a distributed tangential force F_T applied along the circle θ_0
$w_M(\theta,\theta_0), w_R, w_T$ = radial velocity component of shell response at field point θ to, respectively, distributed moment excitation M, distributed radial force F_R, and distributed tangential force F_T applied along circle θ_0
$\bar{w}_M, \bar{w}_R, \bar{w}_T, \bar{u}_T$ = mechanical admittances, defined, respectively, as w_M/M, w_R/F_R, w_T/F_T, u_T/F_T
Z, Z_T = modal impedance of spherical shells, respectively, for radial and tangential excitation
Z_p = drive-point impedance of infinite flat plate $= 8\beta\rho ch a$
α = circular frequency of excitation normalized with respect to the flexural wavelength, $\equiv \omega a/c_f = (\Omega/\beta)^{1/2}$
$\beta = h/2\sqrt{3}a$
η = loss factor of shell material
θ = spherical polar angle defining degree of latitude of field point
θ_0 = degree of latitude defining cutout boundary or distributed load
$\lambda = n(n+1)$
μ = Poisson's ratio
ρ = density of shell material
$\Phi(\theta_0), \Psi(\theta_0)$ = dimensionless generalized forces defined in (35)
Ω = dimensionless frequency of excitation normalized with respect to the compressional wavelength in a flat plate, or the electromagnetic velocity in Watson's problem, $\equiv \omega a/c$
ω = circular frequency of excitation

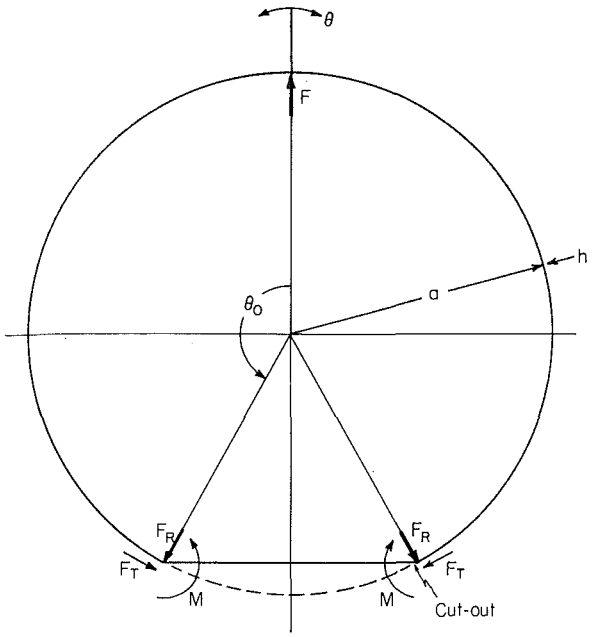

Fig. 2 Spherical shell point-excited at $\theta = 0$ and subject to axisymmetric constraints at θ_0

formulation yields more immediate insight into the phenomena of, respectively, diffraction or high-frequency shell vibrations than does a slowly converging wave-harmonic or normal-mode series. The drive-point impedance tends to that of the infinite plane plate as $\alpha\eta \to \infty$. Watson's solution thus provides an intellectually satisfying transition from the finite to the infinite system. This closed-form nonmodal formulation of structural response by means of progressive or standing waves was systematically applied by Snowdon [8] for beams and by Skudrzyk [9] for plates. The present paper extends the creeping-wave formulation of the complete spherical shell [6] to a shell provided with a circular cutout located coaxially with the drive point, Fig. 2. The asymptotic approximations and the functional dependence of shell response on shell parameters and frequency are generally consistent with Ross' asymptotic analysis of higher-order resonances of an incomplete spherical shell [10].

For the incomplete sphere, the use of a modal expansion at high frequencies is even more cumbersome than for the closed shell because of the additional task of matching boundary conditions. In the present standing or propagating-wave solution, the boundary conditions can be matched by the procedure developed for two-dimensional acoustic or electromagnetic scattering and reflection phenomena. For a shell with standard cutout boundary conditions, whereby all of the incident structure-borne energy is reflected by the boundary, a standing-wave formulation in terms of trigonometric functions, (2), is convenient. When the cutout defines the intersection of two shells, or of a wave guide attached to a spherical shell, a traveling-wave representation of the hypergeometric function (2) in terms of exponentials permits a simple wave-guide-type analysis. The propagating-wave solution of the complete spherical shell will first be summarized. Nearly the same Nomenclature is used here and in [6].

The radial velocity distribution of a spherical shell excited by a concentrated force applied at $\theta = 0$ is conveniently expressed in terms of the impedances $Z(\Omega, \lambda)$ of the normal modes:

$$w_p(\theta) = \frac{F}{2\pi a^2} \sum_{n=0}^{\infty} \frac{(n + \frac{1}{2})P_n(\cos\theta)}{Z(\Omega, \lambda)} \tag{3}$$

where

$$Z(\Omega, \lambda) \approx \frac{i2\sqrt{3}\beta\rho c}{\Omega} (\beta^2\lambda^2 - \Omega^2) + 0(\Omega^{-2}) + 0(\beta^2) \tag{4}$$

The corresponding tangential velocity is, with the same high-frequency, thin-shell approximations

$$u_p(\theta) \approx \sum_{n=1} \frac{\beta^2\lambda + 1 + \mu}{\lambda - \Omega^2} W_n P_n^1(\cos\theta) \tag{5}$$

where W_n is a modal velocity amplitude in the normal-mode series (3).

This normal-mode series lends itself to the Sommerfeld-Watson transformation. The two roots of the modal impedances (4), $\lambda_j = \pm\Omega/\beta \equiv \pm\alpha^2$ each give rise to two roots s_j

$$\left.\begin{aligned} s_{1,2} &\approx \pm\alpha \\ s_{3,4} &\approx \pm i\alpha \end{aligned}\right\} + 0(1/8\alpha) \tag{6}$$

The roots s_1 and s_3 which fall within the contour $(C_2 + C_{R+} + C_3)$, give rise to two residues. When the hypergeometric functions are replaced by their asymptotic expressions (2) and dropping higher-order terms in α^{-2}, one finally obtains a concise solution

$$w_p(\theta) = \frac{-iFf(\theta)}{Z_p(\pi\alpha \sin\theta)^{1/2}}, \qquad \theta \neq 0, \pi \tag{7}$$

where

$$f(\theta) \equiv 2^{1/2}\left(\frac{\cos\left[\alpha(\pi - \theta) - \frac{\pi}{4}\right]}{\cos\alpha\pi} - \frac{e^{-i\pi/4}\cos\left[i\alpha(\pi - \theta) - \frac{\pi}{4}\right]}{\cosh\alpha\pi}\right) \tag{8}$$

$$= (1 + \tan\alpha\pi)\cos\alpha\theta - (1 - \tan\alpha\pi)\sin\alpha\theta - 2^{1/2}e^{-\alpha\theta} + 0(e^{-\pi\alpha})$$

The exponential term represents a nonpropagating near-field beyond which the standing or propagating-wave nature of the residue associated with s_1 can be displayed by expressing the trigonometric functions in terms of complex exponentials. The corresponding phase velocity obtained by retaining a higher-order term in (6) is

$$\begin{aligned} c_1 &= \omega a/s_1 \\ &= c_f\left[\left(1 - \frac{1}{8\alpha^2}\right) + 0(\alpha^{-4})\right] \end{aligned} \tag{9}$$

This velocity displays the "creeping-wave" characteristics of the diffracted-wave solution. Similarly, for a tangential excitation, the phase velocity in the shell is somewhat less than the compressional velocity in a flat plate. At the drive point a slightly modified version of the Watson transformation, not applicable to diffraction problems, yields

$$w_p(0) = -i(F/Z_p)\tan\alpha\pi \tag{10}$$

To evaluate the order of magnitude of the associated tangential response the ratio multiplying W_n in (5) is evaluated for the singular values of $\lambda_j = \pm\alpha^2$:

$$\frac{U_n}{W_n} = \frac{1 + \mu}{\pm\alpha^2} + 0(\beta^2) \tag{11}$$

where U_n is the modal velocity amplitude multiplying P_n^1 in (5). The asymptotic expression of this function is obtained by differentiating (2). Setting $n = s - \frac{1}{2}$,

$$\begin{aligned} P_{s-\frac{1}{2}}^1(\cos\theta) &= -dP_{s-\frac{1}{2}}/d\theta \\ &\approx -\frac{(2s)^{1/2}}{(\pi \sin\theta)^{1/2}}\sin\left(s\theta - \frac{\pi}{4}\right), \qquad |s|\sin\theta \gg 1 \end{aligned} \tag{12}$$

This function exceeds the original hypergeometric function, (2), by a factor $s = \alpha$. Combining (11) and (12) it is seen that the tangential displacements compare to the radial displacements as α^{-1} compares to unity, and can therefore be neglected, provided the excitation is purely radial.

Having reviewed the results obtained in [6] for the point-excited spherical shell the response to circular line loads will be derived.

2 Shell Response to Distributed Forces and Moments

Distributed Radial Load. A radial force of resultant amplitude of F_R is applied uniformly around the circle of latitude θ_0. The intensity of the line load in units of force per unit length is $F_R/2\pi a \sin \theta_0$. The corresponding applied pressure is in the form of a Dirac delta function which is readily expanded in Legendre functions

$$p_a(\theta_0) = \frac{F_R \delta(\theta - \theta_0)}{2\pi a^2 \sin \theta_0} = \frac{F_R}{2\pi a^2} \sum_{n=0}^{\infty} (n + \tfrac{1}{2}) P_n(\cos \theta_0) \tag{13}$$

The modal formulation of the radial velocity distribution thus excited is

$$w_R(\theta, \theta_0) = \frac{F_R}{2\pi a^2} \sum_{n=0}^{\infty} \frac{(n + \tfrac{1}{2}) P_n(\cos \theta_0) P_n(\cos \theta)}{Z(\Omega, \lambda)} \tag{14}$$

To generate the Watson residue series, we note that, according to (1a) the normal-mode series equals the contour integral $(C_1 + C_2)$

$$\sum_n = -\frac{i}{2} \oint_{C_1 + C_2} \frac{F(s, \pi - \theta, \theta_0) s ds}{Z(\Omega, \lambda)} \tag{15a}$$

where

$$F(s, \pi - \theta, \theta_0) \equiv P_{s-\frac{1}{2}}(\cos \theta_0) P_{s-\frac{1}{2}}(-\cos \theta)/\cos s\pi$$

This integrand, like Watson's integrand (1a) is odd in s, so that the clockwise integral $(C_1 + C_2)$ equals the line integral $(C_3 + C_2)$ from $-\infty$ to ∞. Unlike Watson's diffraction analysis or the point-excited spherical shell solution [6], for which $\theta > \theta_0 = 0$, the present analysis must include the situation $\theta < \theta_0$. It will shortly become apparent that this requires an alternative integral representation based on the fact that, since the integrand in (15a) is odd in s, the line integral C_2 from 0 to ∞ equals its mirror image C_4 from 0 to $-\infty$. Hence, the clockwise integral $(C_1 + C_2)$ equals alternatively the line integral $(C_3 + C_2)$ from $-\infty$ to ∞ above the real axis or the line integral $(C_1 + C_4)$ from ∞ to $-\infty$ below the real axis. The latter must be closed along the semicircular circle C_{R-} to exclude the poles on the real axis.

To determine where these alternative integral representations are applicable, one studies the behavior of the integrand on the two semicircular contours as $|s| \to \infty$:

$$\sum_n = -\pi \sum_{s=s_j} \frac{sF(s, \pi - \theta, \theta_0)}{\partial Z/\partial s}, \begin{cases} \mathrm{Im}(s_j) > 0, & \theta > \theta_0 \\ \mathrm{Im}(s_j) < 0, & \theta < \theta_0 \end{cases} \tag{15b}$$

At $\theta = \theta_0$, either representation can be used, because the exponential terms equal unity, and F converges with increasing s as s/Z, i.e., as s^{-3}. Whatever the sign of $(\theta - \theta_0)$, the response is in the form of one of the two pairs of residues associated with the four singularities in (6), the residues being multiplied by the value of $P_{s-\frac{1}{2}}(\cos \theta_0)$ evaluated at $s = s_j$ and s_k:

$$w_R(\theta, \theta_0) = \frac{-iF_R}{Z_p} [F(s_j, \pi - \theta, \theta_0) - F(s_k, \pi - \theta, \theta_0)] \tag{16}$$

where

$$s_j = s_1 \approx \alpha \quad \text{and} \quad s_k = s_3 \approx i\alpha \quad \text{for} \quad 0 \leq \theta_0 < \theta \leq \pi$$

$$s_j = s_2 \approx -\alpha \quad \text{and} \quad s_k = s_4 \approx -i\alpha \quad \text{for} \quad \pi \geq \theta_0 > \theta > 0.$$

The former of the foregoing solutions applies to the response at $\theta = \pi$, where the hypergeometric functions of argument $-\cos \theta$ are unity, but neither solution yields the response at $\theta = 0$. It is not necessary, as it was in the case of the concentrated force, to introduce a modified Watson transformation specialized to this field point. Rather, it is sufficient to note that an integral representation in the upper half of the s-plane can be retained if, instead of the integrand used in (15a) one introduces the function $F(s, \theta, \pi - \theta_0)$. This approach is based upon the fact that the response at $\theta = 0$ to a ring load applied at θ_0 equals the response at $\theta = \pi$ to a ring load applied at $\pi - \theta_0$. Setting $\cos(\pi - \theta_0) = -\cos \theta_0$, the drive-point response becomes

$$w_R(0, \theta_0) = \frac{-iF_R}{Z_p} \left(\frac{P_{s-\frac{1}{2}}(-\cos \theta_0)}{\cos s\pi} \bigg|_{s=s_1} - \frac{P_{s-\frac{1}{2}}(\cos \theta_0)}{\cos s\pi} \bigg|_{s=s_2} \right) \tag{17}$$

To obtain a readily evaluable form of the foregoing solutions, the same high-frequency approximations are introduced as for the point-excited shell. Furthermore, because the functions in (16) and (17) are even in s, the residues arising from s_2 and s_4 are, respectively, the same as for s_1 and s_3, provided one uses the absolute value of the difference $|\theta_0 - \theta|$. The shell response to the ring load, expressed in the form of a transfer admittance can thus be stated as

$$\bar{w}_R(\theta, \theta_0) \equiv w_R(\theta, \theta_0)/F_R = -ig(\theta, \theta_0)/\pi Z_p \alpha (\sin \theta \sin \theta_0)^{1/2}, \quad \theta \neq 0, \pi \tag{18}$$

where

$$g(\theta, \theta_0) \equiv \cos \alpha(\theta_0 + \theta) - \sin \alpha|\theta_0 - \theta| + \tan \alpha\pi [\cos \alpha|\theta_0 - \theta| + \sin \alpha(\theta_0 + \theta)] - \exp[-\alpha|\theta_0 - \theta|] + 0(e^{-\alpha\theta_0})$$

The solution at the origin $\theta = 0$ (17) takes a simple form expressible in terms of the function $f(\theta)$ defined in (8):

$$\bar{w}_R(0, \theta_0) = -if(\theta_0)/Z_p(\pi\alpha \sin \theta_0)^{1/2} \tag{19}$$

where terms of order $\exp(-\alpha\theta_0)$ were neglected compared to $f(\theta_0)$.

Distributed Moment Load. The shell response to a moment is obtained by superimposing the response to a positive, outward, radial force F_R applied at θ_0 and the response to a negative inward radial force of the same amplitude applied at $(\theta_0 + \delta\theta_0)$. The two forces thus form a positive moment

$$M = F_R a \delta\theta_0$$

The residue series representing the shell response to this moment can be constructed from (16) and (17) by replacing the hypergeometric functions of argument $\cos \theta_0$ with

$$P_{s-\frac{1}{2}}(\cos \theta_0) - P_{s-\frac{1}{2}}[\cos(\theta_0 + \delta\theta_0)] = -(dP_{s-\frac{1}{2}}/d\theta_0)\delta\theta_0$$

Setting $\delta\theta_0 = M/F_R a$, one constructs the desired solution of the shell response to a distributed moment by differentiating (16):

$$w_M(\theta, \theta_0) = -(M/a)\partial\bar{w}_R(\theta, \theta_0)/\partial\theta_0, \quad \theta \neq 0 \tag{20a}$$

The response at $\theta = 0$ is similarly constructed from (17) but because the argument of the hypergeometric function is $\cos(\pi - \theta_0)$, rather than $\cos \theta_0$, the moment is represented by $-F_R a \delta\theta_0$:

$$w_M(0, \theta_0) = (M/a)\partial\bar{w}_R(0, \theta_0)/\partial\theta_0 \tag{20b}$$

Ignoring terms of order α^{-1} compared to unity in performing the differentiation, the asymptotic expression for the shell response is

$$\bar{w}_M(\theta, \theta_0) \equiv \frac{w_M(\theta, \theta_0)}{M} = \frac{i\partial g(\theta, \theta_0)/\partial\theta_0}{\pi a \alpha Z_p (\sin\theta \sin\theta_0)^{1/2}}, \qquad \theta \neq 0, \pi \tag{21a}$$

where

$$\frac{\partial g(\theta, \theta_0)}{\alpha \partial \theta_0} = \cos\alpha|\theta_0 - \theta| - \sin\alpha(\theta + \theta_0)$$
$$+ \tan\alpha\pi[\sin|\theta_0 - \theta| + \cos\alpha(\theta_0 + \theta)] - \exp(-\alpha|\theta_0 - \theta|)$$

At the drive point, the response is constructed from (20*b*)

$$\bar{w}_M(0, \theta_0) = \frac{-idf/d\theta_0}{aZ_p(\pi\alpha \sin\theta_0)^{1/2}} \tag{21b}$$

where, from (8)

$$df/d\theta_0 = -\alpha[(1 + \tan\alpha\pi)\sin\alpha\theta_0 + (1 - \tan\alpha\pi)\cos\alpha\theta_0]$$

Distributed Tangential Force. Finally, the response of the shell to a distributed tangential load is required for certain boundary conditions. The resultant force is defined as F_T. The corresponding applied shear stress can be expanded in a series of associated Legendre function

$$t_a(\theta_0) = F_T\delta(\theta - \theta_0)/2\pi a^2 \sin\theta_0 = \frac{F_T}{2\pi a^2}\sum_{n=1}^{\infty}\frac{n + \frac{1}{2}}{\lambda}P_n^1(\cos\theta_0) \tag{22}$$

The tangential component of the shell response is

$$u_T(\theta, \theta_0) = \frac{F_T}{2\pi a^2}\sum_{n=1}^{\infty}\frac{(n + \frac{1}{2})P_n^1(\cos\theta_0)P_n^1(\cos\theta)}{\lambda Z_T(\Omega, \lambda)} \tag{23}$$

The subscript T indicates that the tangential displacement is associated with a tangential excitation rather than with coupling to the radial response. Making the usual high-frequency approximations the modal impedance takes the form

$$Z_T = i2\sqrt{3}\beta\rho c(\lambda - \Omega^2)/\Omega \tag{24}$$

The radial response coupled to the tangential response excited by a tangential load will be similarly identified by a subscript T

$$w_T(\theta, \theta_0) = \sum_{n=1}^{\infty}\frac{\lambda(1 + \mu)}{\beta^2\lambda^2 + 2(1 + \mu) - \Omega^2}U_nP_n(\cos\theta) \tag{25}$$

where U_n is the modal velocity amplitude in (23). Applying the Sommerfeld-Watson transformation to the normal-mode series,

$$\sum_n = -\pi\sum_{s=s_j}\frac{sP^1{}_{s-\frac{1}{2}}(\cos\theta_0)P^1{}_{s-\frac{1}{2}}(-\cos\theta)}{\lambda\cos s\pi(\partial Z_T/\partial\lambda)(\partial\lambda/\partial s)} \tag{26}$$

where $Z_T(\Omega, \lambda_j) = 0$, $\lambda_j \equiv (s_j - \frac{1}{2})(s_j + \frac{1}{2})$. The impedance has two, rather than four roots, both of them real

$$s_j = \pm(\Omega^2 + \tfrac{1}{4})^{1/2} \approx \pm\Omega + 0(\Omega^{-2}) \tag{27}$$

Introducing a structural loss factor it is seen that the positive root $s_1 = \Omega(1 + \frac{1}{2}i\eta)$ lies in the upper half plane, while the negative root lies in the lower half plane. A single residue is thus obtained whose denominator is

$$\partial Z_T/\partial s|_{s=s_j} = i4\sqrt{3}\beta\rho c\Omega s_j \tag{28}$$

An explicit expression for the shell response to a tangential load can now be constructed by combining (26) and (28). Introducing the plate impedance Z_p and the parameter β,

$$u_T(\theta, \theta_0) = \frac{-i2\beta F_T}{Z_p\Omega}\frac{P^1{}_{s_j-\frac{1}{2}}(\cos\theta_0)P^1{}_{s_j-\frac{1}{2}}(-\cos\theta)}{\cos s_j\pi}, \begin{cases} j = 1, & \theta > \theta_0 \\ j = 2, & \theta < \theta_0 \end{cases} \tag{29}$$

This solution differs from the one obtained for the radial excitation in that it does not embody a nonpropagating near-field. Introducing (12), the asymptotic expression for the response of the sphere can be written in terms of $|\theta_0 - \theta|$, and $(\theta_0 + \theta)$

$$\bar{u}_T(\theta, \theta_0) \equiv u_T(\theta, \theta_0)/F_T = \frac{-2i\beta}{\pi Z_p \cos\Omega\pi(\sin\theta \sin\theta_0)^{1/2}}\{\sin\Omega|\theta_0 - \theta| + \cos\Omega(\theta_0 + \theta)$$
$$+ \tan\Omega\pi[\sin\Omega(\theta_0 + \theta) - \cos\Omega|\theta_0 - \theta|]\} \tag{30}$$

This function is smaller than $\bar{w}_R(\theta)$ by one order of magnitude, specifically by $0(\alpha/\beta) = 0(\Omega^{1/2}/\beta^{3/2})$. This difference in magnitude reflects the inherently higher impedance of the shell to tangential forces giving rise primarily to membrane stresses. The tangential response at $\theta = 0$ is zero.

The radial response coupled to this tangential velocity distribution is obtained by evaluating the ratio in (25) at the singular value λ_j, where this ratio reduces to $(1 + \mu)$. Differentiating (25) with respect to θ the relation between the two displacement components becomes

$$\partial w_T/\partial\theta = (1 + \mu)u_T \tag{31}$$

For $\mu = 0$, this relation reduces to the condition for a pure membrane-type stress distribution, just as the high-frequency response to radial excitation was found, from (11) and (12), to be asymptotically, purely flexural. The fact that first-order flexural stresses are predicted from (31) for $\mu > 0$ suggests that the μ-term may be the result of an inconsistency in discarding higher-order terms in the equations of motion of the shell. Whether or not this μ-term is retained, one concludes that, unlike the coupling between a radial excitation and a tangential velocity displacement, which was found to be negligible, a tangential excitation makes a contribution to the radial shell response which is comparable to the directly excited tangential shell response. Substituting (29) into (31), and integrating with respect to θ, the coupled radial displacement is finally obtained.

$$\bar{w}_T(\theta, \theta_0) = \frac{-2i\beta(1 + \mu)}{\pi Z_p \cos\Omega\pi}P^1{}_{s_j-\frac{1}{2}}(\cos\theta_0)P_{s_j-\frac{1}{2}}(-\cos\theta)$$

3 Construction of Shell Response From Boundary Condition

The procedure will be illustrated for a cutout with clamped boundary conditions

$$u(\theta_0, \theta_0), w(\theta_0, \theta_0), \left.\frac{\partial w(\theta, \theta_0)}{\partial\theta}\right|_{\theta=\theta_0} = 0 \tag{32}$$

The tangential component is expressed in terms of an unknown tangential reaction along the boundary and a higher-order component coupled to the radial displacement

$$u(\theta, \theta_0) = \bar{u}_T(\theta, \theta_0)F_T + 0(w_R/\alpha) \tag{33a}$$

The radial response is the sum of four terms, three of which are proportional to the unknown reactions along the boundary

$$w(\theta, \theta_0) = w_p(\theta, \theta_0) + \bar{w}_R(\theta, \theta_0)F_R + \bar{w}_T(\theta, \theta_0)F_T + \bar{w}_M(\theta, \theta_0)MI \tag{33b}$$

The slope $\partial w/\partial\theta$ of the radial velocity is made up of these same components. In the large α-limit the coupling term in (33*a*) is negligible. Consequently, the first of the boundary equations (32) yields $F_T = 0$. When this is substituted in the latter two boundary conditions one obtains two linear equations in the unknown radial and moment reaction along the boundary. These two simultaneous equations yield formal solutions expressible in terms of the results obtained in section 2

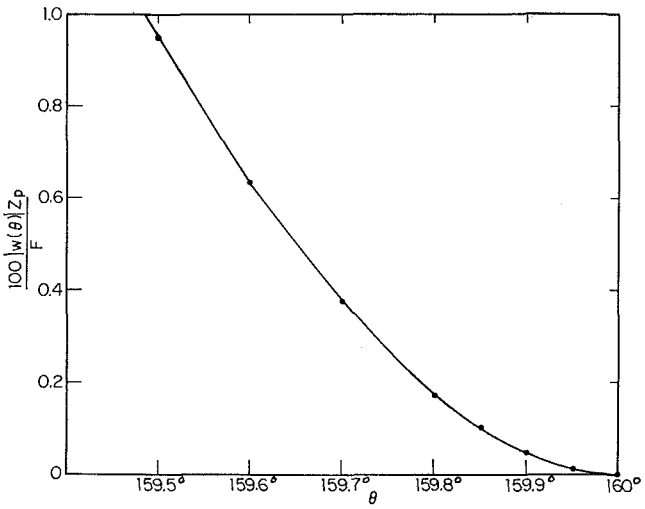

Fig. 3 Radial response of spherical shell in vicinity of cutout for same parameters as in Table 1

$$\left.\begin{aligned} F_R &= \frac{w_p'\bar{w}_M - w_p\bar{w}_M'}{\bar{w}_R\bar{w}_M' - \bar{w}_M\bar{w}_R'} \\ M &= \frac{w_p\bar{w}_R' - w_p'\bar{w}_R}{\bar{w}_R\bar{w}_M' - \bar{w}_M\bar{w}_R'} \end{aligned}\right\} \quad \begin{aligned} &\text{where } w_p \equiv w_p(\theta_0, \theta_0) \\ &w_p' \equiv \partial w_p/\partial\theta|_{\theta=\theta_0} \\ &\bar{w}_R \equiv \bar{w}_R(\theta_0, \theta_0) \\ &\text{etc.} \end{aligned} \tag{34}$$

The solutions of the two simultaneous equations can be expressed in terms of (8), (18), and (21a)

$$F_R = (\pi\alpha \sin\theta_0)^{1/2}\Phi(\theta_0), \qquad M = -Fa(\pi\alpha \sin\theta_0)^{1/2}\psi(\theta_0) \tag{35}$$

where

$$\Phi(\theta_0) \equiv \frac{fg'' - g'f'}{(g')^2 - gg''}, \qquad \psi(\theta_0) \equiv \frac{gf' - fg'}{(g')^2 - gg''}$$

$$f \equiv f(\theta_0); \quad f' \equiv df(\theta_0)/d\theta_0;$$

$$g \equiv g(\theta_0, \theta_0) = \cos 2\alpha\theta_0 + \tan\alpha\pi(1 + \sin 2\alpha\theta_0) - 1$$

$$g' \equiv \left.\frac{\partial g(\theta, \theta_0)}{\partial\theta_0}\right|_{\theta=\theta_0} = \left.\frac{\partial g(\theta, \theta_0)}{\partial\theta}\right|_{\theta=\theta_0} = \alpha(\tan\alpha\pi \cos 2\alpha\theta_0 - \sin 2\alpha\theta_0)$$

$$g'' \equiv \partial^2 g/\partial\theta\partial\theta_0|_{\theta=\theta_0} = \alpha^2[1 - \cos 2\alpha\theta_0 + \tan\alpha\pi(1 - \sin 2\alpha\theta_0)]$$

$$(g')^2 - gg'' = 2\alpha^2(1 - \cos 2\alpha\theta_0 - \tan\alpha\pi \sin 2\alpha\theta_0)$$

Finally, the response of the shell is constructed by substituting these results in (33b) where the velocity components have been expressed explicitly in terms of (8), (18), (19), and (21)

$$w(\theta, \theta_0) = \frac{-iF}{Z_p(\alpha\pi \sin\theta)^{1/2}}\left[f(\theta) + \Phi(\theta_0)g(\theta, \theta_0) + \psi(\theta_0)\frac{\partial g(\theta, \theta_0)}{\partial\theta_0}\right], \qquad \theta \neq 0 \tag{36a}$$

$$w(0, \theta_0) = \frac{-iF}{Z_p}\left[\tan\alpha\pi + \Phi(\theta_0)f(\theta_0) - \psi(\theta_0)\frac{df(\theta_0)}{d\theta_0}\right] \tag{36b}$$

Because of the uniqueness of the solution, the result thus obtained describes the response of a point-excited shell subject to the prescribed boundary conditions, as well as the response of a complete shell driven by the point-force F and the distributed excitations F_R and M. Had the higher-order term in (33a) been retained, a nonvanishing value for F_T would have resulted, requiring the use of third instead of the second-order determinants in the evaluation of the reactions along the boundary.

The solution in (36) is used to compute the response of a shell

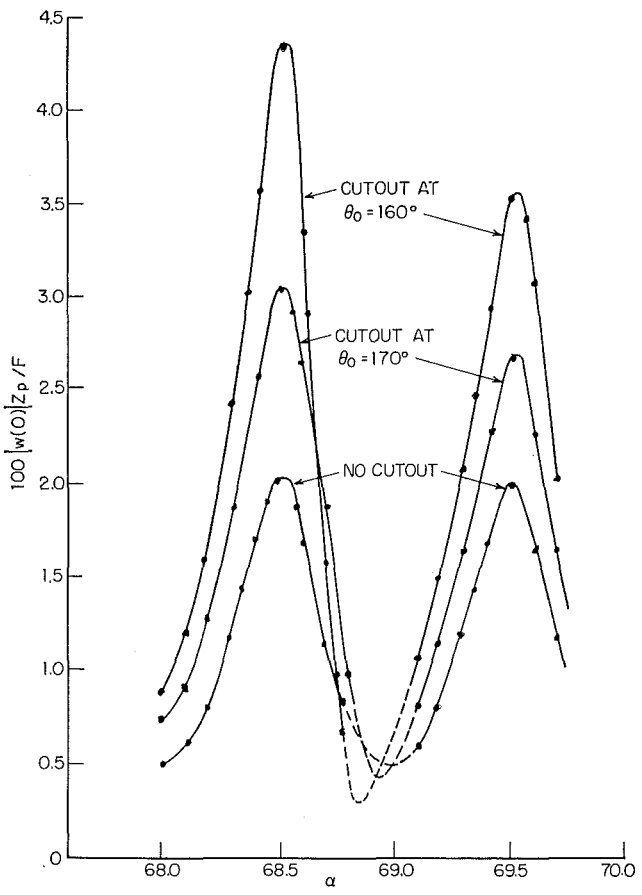

Fig. 4 Resonance peaks of spherical shells with cutouts at θ_0 = 160 deg and 170 deg and for a complete spherical shell excited by a point force applied at θ = 0, ($h/a = 10^{-2}$, η = 0.01)

Table 1 Radial velocity of shell with cutout at θ_0 = 160 deg and of complete shell [6] excited by a radial force F applied at θ = 0 ($h/a = 10^{-2}$, Ω = 13.8, α = 69.1, η = 0.04)

	$100\|w(\theta)\|Z_p/F$		Phase with respect to driving force (deg)	
θ (deg)	Cutout	No cutout	Cutout	No cutout
0	99.5	97.9	−4.3	0.1
2	54.7	54.8	92.5	92.4
5	30.1	30.5	299.5	299.3
10	20.4	20.5	285.3	285.1
20	13.1	12.9	258.1	256.6
50	5.46	5.76	172.0	165.7
90	3.58	3.16	64.8	56.7
130	2.63	2.90	279.2	287.3
150	3.73	2.38	260.5	260.6
160	$0(10^{-7})$	1.20	...	247.0
180	...	22.6	...	101.2

for a cutout subtending an angle of 40 deg (i.e., for θ_0 = 160 deg), and for the driving frequency and shell parameters used in the illustration of the wave-guide analysis of the complete spherical shell [6], viz., Ω = 13.8, η = 0.04, $h/a = 10^{-2}$, α = 69.1. The radial response of the shell is illustrated in Table 1. The shell response in the immediate vicinity of the cutout is shown in Fig. 3 to verify that the clamped boundary conditions are indeed satisfied.

The results obtained for the complete shell [6] are also reproduced in Table 1. The response of the two shells is mildly similar, except for marked differences at the drive point and in the vicinity of the cutout. The large divergence at the drive point may be attributed to a mild focusing of the wave components contributed by the reactions at the cutout boundaries.

The effect of resonant conditions on the drive-point response is

illustrated in Fig. 4 for more lightly damped shells. The drive-point response oscillates around that of the infinite flat plate. The resonant amplification is more pronounced for shells with larger cutouts. To explore the cause of this trend, it is noted that the resonant and antiresonant amplitudes of the complete shell are, respectively,

$$w(0)Z_p/F = \coth(\pi\alpha\eta/4) \text{ at resonance}$$
$$= \tanh(\pi\alpha\eta/4) \text{ at antiresonance}$$

Thus the enhancement at resonance and cancellation at antiresonance are determined by the length of the structure-borne path measured in flexural wavelengths, $2\pi\alpha$, multiplied by $\eta/8$. For shells with cutouts, the effective length of the wave-guide path is $2\alpha\theta_0$ modified by the boundary conditions. An increase in θ_0 from, e.g., 160–170 deg produces a change in the function $\theta_0\alpha\eta/4$ which is equivalent to an increase in α from, e.g., 69–73. These results are consistent with the reduction in resonant response with increasing θ_0 at constant α, and alternatively increasing α at constant θ_0 shown in Fig. 4. As $\theta_0 \to \pi$, the response of shells with clamped cutouts does not converge precisely to the response of the complete free shell, but to that of the complete shell supported at $\theta = \pi$.

The maxima of the response of shells with cutouts coincide with those of the complete shell which occur at the singularity of tan $\alpha\pi$, corresponding to the dimensionless natural frequencies, $\alpha_m = (m + \frac{1}{2})$. These frequencies are also maxima of the two θ_0-dependent components of the drive-point response (36*b*). The denominators of the coefficients $\Phi(\theta_0)$ and $\psi(\theta_0)$ of these two components display zeros when tan $\alpha\theta_0$ = tan $\alpha\pi$, i.e., when $\alpha_m = m\pi/(\pi - \theta_0)$. These roots are, however, also zeros of the numerators of the two functions and therefore do not give rise to resonance peaks. If terms of order exp $(-\alpha\theta_0)$ are not negligible, i.e., for lower frequencies α or for partial shells which are curved plates subtending an angle $\theta_0 < \pi/2$ rather than shells with small cutouts, θ_0-dependent resonances would have been encountered.

For standard boundary conditions, the components of either the velocity or the load along the boundary are zero, i.e., the boundary presents infinite or vanishing admittance to transverse, tangential, and rotational motions. For a spherical shell intersecting another elastic shell along the circle θ_0, the boundary conditions are defined by the requirement that the velocity components and reactions in the two shells along the boundary be compatible. When the attached structure is a semi-infinite wave guide, the input impedance of the receiving structure embodies a resistive component, thus making the boundary into an energy sink. In this situation it is advantageous to display the incident structureborne wave field w_p in terms of complex exponentials, i.e., of traveling waves, even for $\eta = 0$. The structure-borne waves reflected by the boundary are similarly displayed in terms of complex exponentials, exp $[i\alpha|\theta_0 \pm \theta|]$ and exp $[i\Omega|\theta_0 \pm \theta|]$, and real exponentials exp $[-\alpha|\theta_0 \pm \theta|]$, which are multiplied by undetermined complex coefficients. The wave field transmitted to the attached wave guide is similarly expressed. The unknown coefficients in terms of which the reflected and transmitted fields are formulated can be computed from the boundary conditions. The compatibility of boundary velocities and reactions in the two shells is conveniently stated in terms of the input impedances of the two coupled structures, viz., for the spherical shell, the reciprocals of the input admittances $\bar{w}_R$, $\bar{w}_M$, and $\bar{u}_T$. This impedance matching technique is familiar from the analysis of structure-borne noise transmission between discontinuous structures of elementary geometry, e.g., beams coupled to discrete elements and to other beams [8] or an infinite plate coupled to a parallel infinite plate by means of an elastic column or "sound bridge" [11]. The illustration of this procedure transcends the scope of the present paper.

Acknowledgment

This study was supported by Office of Naval Research, Structural Mechanics Program (Code 439). The author is indebted to his colleagues Y.-S. Hsu and Drs. L. G. Copley and D. Feit for useful suggestions and help with the calculations, and to the reviewer for pointing out an error.

References

1 Sommerfeld, A., *Partial Differential Equations*, Academic Press Inc., New York, 1949, Chapter 6, "Problems of Radio."

2 Wait, J. R., *Electromagnetic Waves in Stratified Media*, The Macmillan Company, New York, 1962, pp. 107–113.

3 Senior, T. B. A., *Analytical and Numerical Studies of Back-Scattering Behavior of Spheres*, University of Michigan Report 7030-1-T, Contract AF04(694)-693, June 1965.

4 Harbold, M. L., and Steinberg, B. N., "Direct Experimental Verification of Creeping Waves," *Journal of the Acoustical Society of America*, Vol. 45, 1969, pp. 592–603.

5 Norwood, F. R., and Miklowitz, J., "Diffraction of Transient Elastic Waves by a Spherical Cavity," JOURNAL OF APPLIED MECHANICS, Vol. 34, TRANS. ASME, Vol. 89, Series E, 1967, pp. 735–744.

6 Feit, D., and Junger, M. C., "High-Frequency Response of an Elastic Spherical Shell," JOURNAL OF APPLIED MECHANICS, Vol. 36, TRANS. ASME, Vol. 91, Series E, 1969, pp. 859–864.

7 Feit, D., "High-Frequency Radial Response of an Elastic Cylindrical Shell," paper submitted for publication in JOURNAL OF APPLIED MECHANICS.

8 Snowdon, J. C., *Vibration and Shock in Damped Mechanical Systems*, Wiley, New York, 1968, pp. 151–173 and 200–240.

9 Skudrzyk, E., *Simple and Complex Vibratory Systems*, Pennsylvania State University Press, 1968, pp. 246–256, particularly Fig. 8.3.

10 Ross, E. W., Jr., "Natural Frequencies and Mode Shapes for Axisymmetric Vibration of Deep Spherical Shells," JOURNAL OF APPLIED MECHANICS, Vol. 32, TRANS. ASME, Vol. 87, Series E, 1965, pp. 553–561.

11 Cremer, L., and Heckl, M., *Körperschall*, Springer-Verlag, Berlin, 1967, pp. 419–423.